Cement and Concrete Research 159 (2022) 106882

Contents lists available at ScienceDirect

Cement and Concrete Research

journal homepage: www.elsevier.com/locate/cemconres

Short communication

NO_x uptake capacities and sequestration pathways by hydrated cementitious phases

Qingxu Jin [a,b,*], Samuel N. Lucas [b,c], Yuanzhi Tang [b,d], Kimberly E. Kurtis [b]

[a] Department of Civil and Environmental Engineering, Michigan State University, East Lansing, MI, USA
[b] School of Civil and Environmental Engineering, Georgia Institute of Technology, Atlanta, GA, USA
[c] School of Chemical Engineering, Mississippi State University, Mississippi State, MS, USA
[d] School of Earth and Atmospheric Sciences, Georgia Institute of Technology, Atlanta, GA, USA

ARTICLE INFO

Keywords:
NO_x sequestration
C-S-H
Portlandite
AFm-SO_4
Calcite

ABSTRACT

This study seeks to quantify NO_x sequestration by individual hydrated cementitious phases (C-S-H, AFm-SO_4, and Ca $(OH)_2$), establish a fundamental understanding of the reaction pathways, and reveal the effects of carbonation ($CaCO_3$ and AFm-CO_3). For uncarbonated phases, the highest NO_x uptake was measured in C-S-H, with the produced nitrite/nitrate physically bound on solid surface. For AFm-SO_4, an anion exchange process was observed, where nitrite/nitrate substitute for sulfate and form new AFm-NO_2/NO_3. Ca$(OH)_2$ showed undetectable NO_x uptake, which may be due to the relative low temperature and relative humidity. For carbonated phases, $CaCO_3$ exhibited an improved NO_x uptake compared to uncarbonated phases, with uptake capacity three times higher than that of C-S-H. The result of AFm-CO_3 indicates that carbonation could potentially inhibit the anion exchange process that was observed in AFm-SO_4. These findings provide guidelines for the rational design and optimization of cement-based materials for enhanced NO_x sequestration.

1. Introduction

Nitrogen oxides (NO_x) are one of the primary causes of the formation of tropospheric ozone and urban smog [1]. Together with sulfur oxides (SO_x), NO_x contribute to acid rain, which damages the natural and built environment. Additionally, NO_x impair the human respiratory and visual systems causing a variety of health problems [1]. To address atmospheric NO_x levels, researchers have proposed using nano photocatalytic TiO_2 in cement-based materials [2–4]. The NO_x uptake capacities for both TiO_2-modified and ordinary cementitious materials demonstrate that properly designed cement-based materials can serve as a potential NO_x sink [5,6].

NO_x sequestration in conventional and TiO_2-modified cement-based materials has been theorized as a two-step process: (1) the conversion of NO_x to nitrite (NO_2^-) and/or nitrate (NO_3^-), and (2) the binding of NO_2^- /NO_3^- within the hydrated cementitious phases. The NO_x conversion mechanisms (Step 1) can be summarized in three primary mechanisms:

i. In the presence of TiO_2 photocatalysts, the photocatalytic reactions upon exposure to NO_x and UV light convert NO_x into NO_2^- and NO_3^- [2,7,8];
ii. In the absence of TiO_2 photocatalysts, surface catalyzed heterogeneous reactions, which are intrinsic to cementitious materials, promote the conversion of NO_x to NO_2^- and/or NO_3^- [4,9]. Higher surface area is expected to enhance the reaction [10]. These reactions can also be facilitated by the monolayers of water on the surfaces and within the pore solution in the cementitious materials [4,9] (see below);
iii. The alkalinity intrinsic to cementitious materials also aids in the transformation of NO_x to NO_2^- and NO_3^- through the reactions between NO_x and hydroxyls present in the pore solution [11,12].

In contrast, the binding mechanism(s) (Step 2) are less understood, with only a few studies attempting to elucidate the mechanism(s) [13,14]. For example, Kaja et al. [15] indicated that the presence of capillary pores in cement-based materials with sizes of 10–50 nm could help increase NO_x binding efficiency. Their work also demonstrated that the carbonation of these materials could increase the formation of capillary pores and in turn enhance photocatalytic efficiency for NO_x conversion [15].

To understand the essential pathways for NO_x binding in cementitious materials, direct examinations of the binding mechanisms are

* Corresponding author at: Department of Civil and Environmental Engineering, Michigan State University, East Lansing, MI, USA.
E-mail address: billjin@egr.msu.edu (Q. Jin).

https://doi.org/10.1016/j.cemconres.2022.106882
Received 31 August 2021; Received in revised form 14 May 2022; Accepted 10 June 2022
Available online 15 June 2022

desired, especially for NO_x interactions with individual cementitious phases. The hydrated and carbonated phases present in concrete vary in structure and composition, and each can have different impacts on the mechanism(s), efficiency, and permanency for NO_x binding. It is unclear whether NO_x is bound within the cementitious material as one or multiple N-containing species, or whether it is sequestered within the cementitious matrix as adsorbed species on the surface of cementitious hydrates, substituted into ordered structures, or dissolved in pore solution. The relative permanency of the NO_x binding mechanism is also important to understand [5]. For instance, our previous studies [5,6] demonstrated that different cements (e.g., portland cement versus calcium aluminate cement) with different chemical composition and hydration products could result in different binding mechanisms, which can lead to over- or under-estimation of the material's NO_x uptake capacity. Therefore, such mechanistic information is critical for designing cement-based materials with desired properties and chemical compositions for enhanced NO_x sequestration.

To address the above discussed knowledge gaps, this study investigates the interaction of NO_x with individual cement hydration products in order to understand the roles of different phases in the mechanisms and capacity for NO_x uptake. Three main hydrated phases in portland cement-based materials are synthesized and exposed to NO_x directly, including calcium silicate hydrate (C-S-H), portlandite ($Ca(OH)_2$), and mono-sulfoaluminate (AFm-SO_4). To investigate the effects of carbonation, calcite ($CaCO_3$) and mono-carboaluminate (AFm-CO_3) were selected since these are the most stable carbonated phases in concrete [16]. In cement-based materials during environmental exposure, these two phases result from the natural carbonation of $Ca(OH)_2$ and C-S-H, and AFm phases, respectively. To quantify the NO_x sequestration capacity and evaluate the binding mechanism for each cementitious phase, a combination of wet chemical extraction, ultraviolet-visible spectrophotometry, and ion chromatography is employed. In addition, X-ray diffraction (XRD) is used to identify changes in mineralogy upon NO_x exposure. Understanding the intrinsic NO_x binding capacity of individual cement phases can facilitate the estimation of concrete's potential for NO_x sequestration and the optimization of composition for this function.

2. Material and methods

2.1. Materials

C-S-H was synthesized from triclinic alite (C_3S) and silica fume. C_3S was obtained from Mineral Research Processing (Meyzieu, France) and its purity was determined by quantitative XRD using the Rietveld method to be 95 ± 1.5 %. The silica fume (42,741 Silicon (IV) oxide, amorphous fumed) was obtained from Alfa Aesar (Ward Hill, MA, USA) with stated purity exceeding 95 % and surface area of 300–350 $m^2\ g^{-1}$. Based on well-established stoichiometry of C-S-H [17] and synthesizing methods [18], 5 g of alite and 1.53 g of silica fume were selected to synthesize C-S-H with a C/S ratio of approximately 1.7 with the sample preparation detailed below. Silica fume was first suspended in 250 g of N_2-degassed deionized water (18.2 MΩ·cm) and stirred for three minutes. Alite was then added to the silica suspension and stirred at 23 ± 2 °C for a week, during which the entire setup was sealed by Parafilm to avoid carbonation. The liquid-to-solid ratio is about 50 by weight to ensure complete reaction and to prevent the formation of calcium hydroxide. At the end of reaction, the suspension was filtered using Whatman grade 1 filter paper and the obtained solids were vacuum dried at 23 ± 2 °C and stored in a doubly sealed inert high-density polyethylene (HDPE) bottle prior to NO_x exposure and characterization.

AFm-SO_4 and AFm-CO_3 were synthesized according to the protocol developed by Matschei [19]. AFm-SO_4 was prepared by mixing C_3A (preparation procedure in the next paragraph) and $CaSO_4$ in a 1:1 M ratio in boiling deionized water with water/solid mass ratio of around 20. The slurry was then stirred at 85 °C for two weeks in a sealed polytetrafluoroethylene (PTFE) bottle prior to filtration with Whatman grade 1 filter paper and vacuum-drying. AFm-CO_3 was prepared by mixing C_3A and $CaCO_3$ in a 1:1 M ratio at 23 ± 2 °C with a water/solid mass ratio of around 20. The mixture was stirred in PTFE-bottles for two weeks prior to filtration and vacuum-drying.

C_3A was prepared by combining analytical reagent grade $CaCO_3$ and Al_2O_3 (certified purity of ≥99 %) in a 3:1 M ratio. The powders were dry-mixed, homogenized, and pressed into pellets at a pressure of 10 MPa. The pellets were placed in zirconia grain-hardened platinum crucibles and sintered at 1450 °C in a muffle furnace for a 24-h period. At the end of the sintering routine, the pellets were air quenched. The pelletized, sintered material was finely ground and pelletized once again, and the sintering routine repeated two more times. After preparation, the C_3A was stored in a doubly sealed HDPE bottle at 23 ± 2 °C until use.

$Ca(OH)_2$ was reagent grade (Acros, Thermo Fisher Scientific Pittsburg, PA, USA) with a stated purity exceeding 98 %. $CaCO_3$ was also reagent grade (Alfa Aesar, Ward Hill, MA, USA) with a certified purity of ≥99 %.

2.2. NO_x exposure

Fig. 1 illustrates the NO_x exposure test 'plug-flow' setup based on ISO 22197 [20] and JIS R 1701 Standards [21]. For the test, 1.00 ± 0.01 g of a powdered phase was placed in weighing boats, which resided at the bottom of a borosilicate reactor with both ends sealed with a filter and screw cap. Each phase was tested separately. The NO_x gas is prepared based on the aforementioned standards and comprises 1000 ppb nitric oxide (NO) gas with ultrapure dry air. The gas passed through the photoreactor at a constant flow rate of 1 L min^{-1}. For $Ca(OH)_2$, the NO_x gas contains 1000 ppb nitric oxide gas with N_2 gas to prevent any potential carbonation during the exposure test. The reaction was conducted at 23 ± 2 °C and 50 ± 2 % relative humidity by passing the gas through a humidifier. The samples were continuously exposed to NO_x gas for 5 h to ensure an ultimate NO_x binding capacity has been reached. The inlet gas concentration stayed at 1000 ppb, which was measured by a chemiluminescent NO/NO_2/NO_x analyzer (Model 200A, Teledyne API). Since this study focuses on examining the interaction between NO_x and hydrated cementitious phases, we omit the inclusion of photocatalytic TiO_2 particles and the UV light exposure compared to the previous studies [5,6]. The entire test setup was covered by a black light-blocking canvas to prevent potential interference from ambient light. After NO_x exposure, samples were stored in double sealed plastic bags prior to nitrite/nitrate detection tests. Control samples without NO_x exposure were also tested.

2.3. NO_2^- and NO_3^- detection

The experimental method for detecting NO_2^- and NO_3^- combines wet extraction, UV–vis spectrophotometry, and ion chromatography. The wet chemical extraction was performed by suspending 0.1 g of NO_x-exposed powders in 40 mL anoxic deionized water (18.2 MΩ·cm, purged with N_2 gas for 48 h) in HDPE bottles. The HDPE bottles were wrapped in aluminum foil to prevent ambient light from affecting the reaction. All bottles were placed on a shaker at 150 rpm for 48 h. After the extraction, the suspension was filtered through a 0.45 μm syringe filter and the filtrate was then analyzed for both nitrite and nitrate concentrations. Three replicates for the wet extraction of each NO_x-solid reaction were prepared for each phase for the nitrite and nitrate detection.

Nitrite concentration was determined using a colorimetric assay kit (Roche, Sigma Aldrich, St. Louis, MO, USA) and measured at 540 nm on a UV–vis spectrometer (Cary 60, Agilent, Santa Clara, CA, USA). Nitrate concentration was determined using an ion chromatography unit (Dionex, Sunnyvale, CA) equipped with an Ionpac® AS14A column (4 × 250 mm) combined with an Ionpac® AG14A guard column (4 × 50 mm) and a Dionex ED40 electrochemical detector. The mobile phase used for ion chromatography contained a mixture of 8 mM Na_2CO_3 and 1 mM

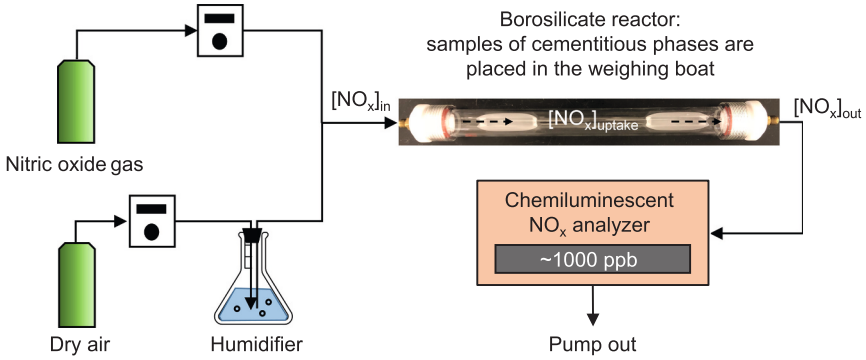

Fig. 1. Experimental setup for NO_x exposure.

$NaHCO_3$, and the flow rate was 0.8 mL min^{-1}.

The total nitrogen (N) mass of NO_x uptake, which was used to represent the measured nitrite and nitrate masses, was determined using Eqs. (1)–(4). For the purpose of comparison, the specific NO_x uptake is normalized by sample mass (this method has been previously demonstrated and validated in refs [5,6]) and with a unit of mg N per kg solid and is denoted as mg kg^{-1} for simplicity.

$$m_{NO_2^-} = C_{NO_2^-} \times DF \quad (1)$$

$$m_{NO_3^-} = C_{NO_3^-} \times DF \quad (2)$$

$$m'_N = m_{NO_2^-} \times \frac{M_N}{M_{NO_2^-}} \quad (3)$$

$$m''_N = m_{NO_3^-} \times \frac{M_N}{M_{NO_3^-}} \quad (4)$$

where $M_{NO_2^-}$ = the mass of nitrite (mg kg^{-1}), $M_{NO_3^-}$ = the mass of nitrate (mg kg^{-1}), $C_{NO_2^-}$ = the concentration of nitrite measured by UV–vis spectrometer (ppm), $C_{NO_3^-}$ = the concentration of nitrate measured by ion chromatography (ppm), DF = dilution factor used for wet chemical extraction (400), m'_N = the mass of nitrogen from nitrite (mg kg^{-1}), m''_N = the mass of nitrogen from nitrate (mg kg^{-1}), $M_{NO_2^-}$ =the molar mass of nitrite = 46 g mol^{-1}, and $M_{NO_3^-}$ =the molar mass of nitrate = 62 g mol^{-1}.

2.4. X-ray diffraction

XRD was performed on the synthetic cementitious phases before and after NO_x exposure to identify changes in mineralogy. Approximately 0.2 g of powders were packed into a sample holder, and the measurements were taken on a PANalytical Empyrean X-ray diffractometer (Malvern Panalytical Ltd., Malvern, United Kingdom) with Cu Kα (λ = 1.54 Å) radiation at 45 kV and 40 mA. Scans were performed at 5–45° 2θ using a PIXcel3D detector and analyzed with PANalytical HighScore Plus software.

3. Results

To understand the pathways for NO_x sequestration, quantify NO_x uptake capacity by each cementitious phase, and understand the effect of carbonation on NO_x uptake, five synthetic cementitious phases that are common in cementitious materials were synthesized and subjected to NO_x exposure under the same conditions. The phases include calcium silicate hydrate (C-S-H), portlandite ($Ca(OH)_2$), mono-sulfoaluminate (AFm-SO_4), calcite ($CaCO_3$), and mono-carboaluminate (AFm-CO_3). NO_x uptake capacity was measured by a combination of wet chemical extraction, UV–vis spectrophotometry, and ion chromatography.

The NO_x conversion results of the measured N mass, combined from NO_2^- and NO_3^- detection, are shown in Fig. 2. Control samples without NO_x exposure showed no detectable NO_2^- or NO_3^-. Based on the combined results from NO_2^-/NO_3^- production and XRD analysis, the binding mechanism and NO_x sequestration pathways for each cementitious phase are considered below.

3.1. Calcium silicate hydrate (C-S-H)

Among three uncarbonated cementitious phases (C-S-H, $Ca(OH)_2$, and AFm-SO_4), C-S-H shows the highest NO_x uptake capacity (calculated as the total amount of nitrite- and nitrate-N produced, Section 2.3), with nitrite measured at approximately 50 mg kg^{-1} and nitrate at 150 mg kg^{-1} (Fig. 2). The presence of higher nitrate concentration compared to nitrite concentration agrees with prior measurements on cement pastes [9]. A relatively high level of NO_x uptake by C-S-H was expected because of the high surface area and the interlayer water molecules that promote heterogeneous catalytic reactions [17,22]. These relate to mechanism (ii), as described in the introduction. Additionally, gel pores are intrinsic to the C-S-H structure and typically contains alkaline pore solution [17,22], which suggests the potential for the formation of NO_2^- and NO_3^- ions [11] via mechanism (iii). Therefore, this study supports the hypothesis of our previous studies [5,10] that C-S-H, with its unique microstructural features, is favorable to NO_x conversion and plays a major role in sequestering NO_x in OPC-based cementitious materials. However, the capacity of C-S-H to bind NO_x has not been previously quantified.

XRD analysis did not observe the formation of new peaks in samples with NO_x exposure (Fig. 3). Given the amount of NO_x sequestered by this phase, this indicates that the formation of new solid phases between C-S-

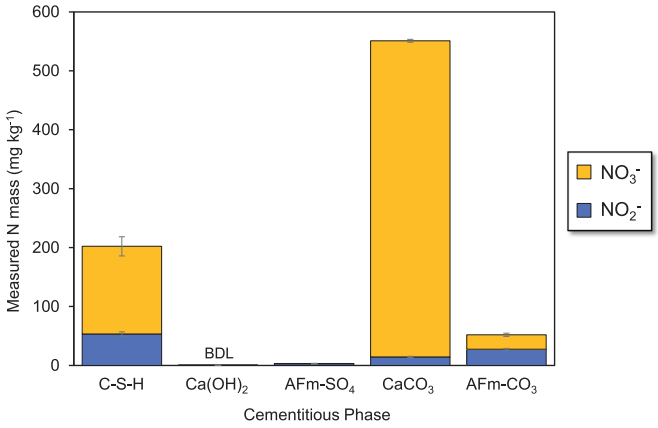

Fig. 2. Measured N mass as nitrite (NO_2^-, blue) or nitrate (NO_3^-, yellow) normalized by sample mass after the reaction of five synthetic cementitious phases with NO_x. The phases include calcium silicate hydrate (C-S-H), portlandite ($Ca(OH)_2$), mono-sulfoaluminate (AFm-SO_4), calcite ($CaCO_3$), and mono-carboaluminate (AFm-CO_3). BDL: below detection limit.

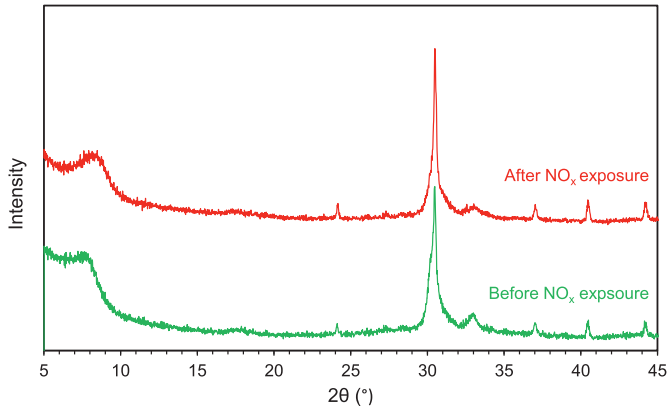

Fig. 3. XRD patterns of C-S-H phases before (control) and after NO_x exposure indicating that the formation of new solid phases between C-S-H and NO_2^- and NO_3^- ions is unlikely because no new peaks or humps (indicative of new crystalline or amorphous phases, respectively) are detected.

H and NO_2^- and NO_3^- ions is unlikely or only at minor amount below the detection limit (the detection limit of XRD for crystalline phase is typically around 5 %). The results also support the previously proposed hypothesis that NO_2^- and NO_3^- likely adsorb on the surface of C-S-H [10,15,23] or dissolve in the pore solution [10]. Either way, these ions are susceptible to wet chemical extraction and can be quantified by UV–vis spectrophotometry and ion chromatography. However, future studies are necessary to discern the relative significance of these two factors in NO_x binding of C-S-H. For synthetic C-S-H, its surface area and morphology are not significantly affected by the Ca/Si ratio but governed by the lime concentration of C-S-H suspension [24,25]. Therefore, the effect of lime concentration should also be considered in the future study for the NO_x uptake in C-S-H.

3.2. Portlandite ($Ca(OH)_2$)

$Ca(OH)_2$ showed no detectable NO_x uptake (Fig. 2), and no new phases were detected by XRD after NO_x exposure (Fig. 4). These results indicate that $Ca(OH)_2$ could be intrinsically resistant to NO_x sequestration, at least under the current experimental conditions. Interestingly, Zhang et al. [26] demonstrated atmospheric NO_x removal by $Ca(OH)_2$. They suggested the following reactions for the interaction of $Ca(OH)_2$ with produced nitrate and nitrate to form calcium nitrite and nitrate:

$$Ca(OH)_2 + 2HNO_2 \rightarrow Ca(NO_2)_2 + 2H_2O \quad (5)$$

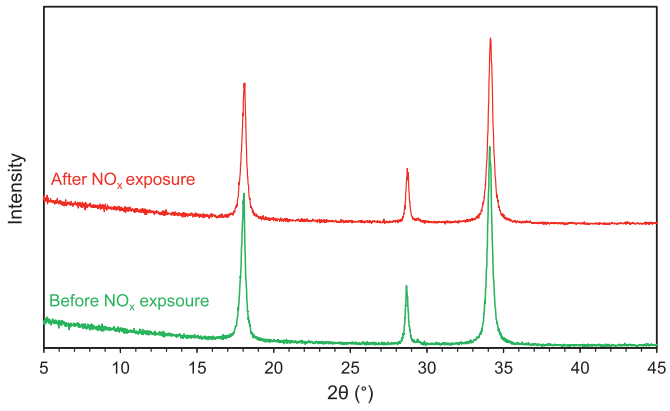

Fig. 4. The XRD patterns of $Ca(OH)_2$ phases before (control) and after NO_x exposure indicates that $Ca(OH)_2$ under the current temperature and relative humidity conditions in this study could be resistant to NO_x uptake because no new peaks (indicative of new crystalline) are detected.

$$Ca(OH)_2 + 2HNO_3 \rightarrow Ca(NO_3)_2 + 2H_2O \quad (6)$$

Because $Ca(NO_2)_2$ and $Ca(NO_3)_2$ are highly soluble, the resulting NO_2^- and NO_3^- ions should be detectable through wet chemical extraction such as that used in our study. However, their experiments were performed at 70 °C and a relative humidity of 60 % [26], which, as the authors proposed, makes nitrous and nitric acid close to liquid-phase steam; the authors did not conduct tests under ambient temperature for comparison. Chen et al. [27] showed SO_2 and NO_x removal by $Ca(OH)_2$ and concluded that the presence of SO_2 could enhance the efficiency of NO_x removal. However, their test was also carried out at a high temperature (70 °C) with a $Ca(OH)_2$ slurry that was pre-treated with water at H_2O/CaO ratio of 5 [27]. Therefore, the inability of $Ca(OH)_2$ to sequester NO_x in this study is likely related to the use of lower temperature and relative humidity (temperature of 23 ± 2 °C and relative humidity of 50 ± 2 %), which are in fact representative of field conditions for much of the world's concrete infrastructure. Further studies are warranted to examine the influence of temperature and relative humidity on the potential for NO_x interaction with $Ca(OH)_2$.

3.3. Mono-sulfoaluminate (AFm-SO_4)

AFm-SO_4 shows significantly lower NO_x uptake compared to C-S-H but does exhibit some capacity for sequestering NO_x. Approximately 3 mg kg^{-1} of nitrite is measured by wet-chemical extraction while no detectable nitrate is measured (Fig. 2).The XRD pattern for AFm-SO_4 before and after NO_x exposure has been previously reported in Jin et al. [6] and is reproduced in Fig. 5. Two new peaks at 9.5° and 15.1° 2θ were observed. According to Glasser et al. [29], the newly formed peaks represent the formation of AFm- NO_2/NO_3. Thermodynamically, it has been demonstrated that NO_2^- and NO_3^- have a binding preference within AFm phases, with a preference of $NO_3^- > NO_2^- > SO_4^{2-} > OH^-$ [30]. Therefore, the result provides direct evidence that NO_3^- and/or NO_2^- can substitute SO_4^{2-} in AFm phase in a solid-gas anion exchange reaction and form crystalline AFm-NO_2/NO_3. The lower amount of nitrate detected by wet chemical extraction than nitrite suggest potential preferable binding of nitrate in AFm phase because the anion exchange process of nitrate took precedence over nitrite [30]. Overall, as discussed in Jin et al. [6], this detection provides further insights that aluminate-rich cementitious materials, with their aluminate-bearing phases, could bind NO_x more permanently through this anion exchange process.

3.4. Calcite ($CaCO_3$)

Carbonation is inevitable in cementitious materials, and the most stable carbonation product of both $Ca(OH)_2$ and C-S-H is calcite [31].

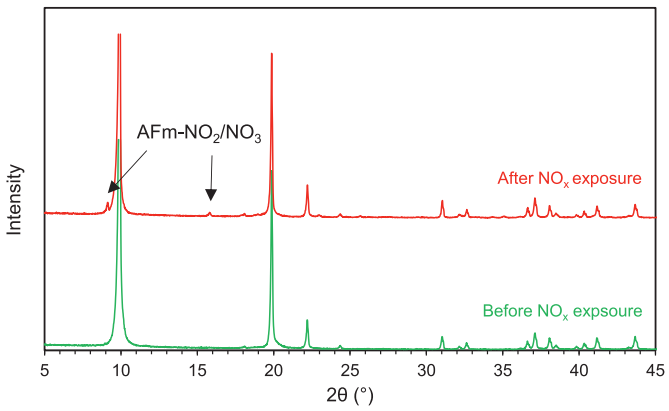

Fig. 5. Two new peaks at 2θ of 9.5° and 15.1° were observed in the XRD patterns of AFm-SO_4 phases before (control) and after NO_x exposure, indicating the formation of AFm- NO_2/NO_3 phases due to NO_x uptake [6].

Thus, this study also examined the effects of carbonation on NO_x sequestration capability. As shown in Fig. 2, calcite exhibits NO_x uptake capacity while portlandite exhibits undetectable NO_x uptake. This result indicates that under current environmental conditions (23 ± 2 °C and relative humidity of 50 ± 2 %) carbonation improves the NO_x uptake capability of portlandite. Similar observation of NO_x uptake by the mineral calcite was reported by Grassian [9] under a relative humidity of 20 %, where NO_x was converted into the gas-phases HNO_3 which further reacted with calcite to form $Ca(NO_3)_2$.

$$CaCO_3 + 2HNO_3 \rightarrow Ca(NO_3)_2 + CO_2 + H_2O \quad (7)$$

Compared to C-S-H, calcite also exhibits a higher NO_x uptake capacity (Fig. 2). As discussed in Section 3.1, the converted NO_2^- and NO_3^- likely adsorb on the surface of C-S-H or dissolve in the pore solution. The higher NO_3^- uptake suggests that the chemical reactions between gas-phases HNO_2/HNO_3 and $CaCO_3$ are more effective in NO_x uptake than the binding mechanism of C-S-H.

According to Fig. 2, the total NO_x uptake of calcite comprises nitrite of approximately 14 mg kg^{-1} and nitrate of 540 mg kg^{-1}, with NO_2^--to-NO_3^- ratio of 1:38. Therefore, it is expected that a small amount of NO_x has converted to gas-phases HNO_2 and reacted with calcite in a similar manner as gas-phases HNO_3 [9], which is described in Eq. (8). The significantly higher concentrations of NO_3^- compared to NO_2^- suggests that under the current environmental conditions the heterogeneous surface-related reactions of calcite seem to favor the formation of $Ca(NO_3)_2$.

$$CaCO_3 + 2HNO_2 \rightarrow Ca(NO_2)_2 + CO_2 + H_2O \quad (8)$$

XRD was also performed to examine the formation of $Ca(NO_2)_2$ and $Ca(NO_3)_2$. Interestingly, no noticeable new peaks were detected by XRD (Fig. 6). This is possibly due to the highly hygroscopic nature of the formed $Ca(NO_2)_2$ and $Ca(NO_3)_2$. Instead of using XRD, Grassian [9] used Fourier-transform infrared spectroscopy (FTIR) and transmission electron microscopy (TEM) to confirm the formation of $Ca(NO_3)_2$. In addition, they also discovered an increased formation of a water layer on the surface of reacted calcite, which further promotes NO_x adsorption and the formation of $Ca(NO_3)_2$.

3.5. Mono-carboaluminate (AFm-CO_3)

The effect of carbonation of AFm on NO_x uptake was examined using AFm-CO_3 as the mono-carboaluminate is the most stable carbonated AFm phase in concrete [16]. Compared to AFm-SO_4, higher amounts of NO_2^- and NO_3^- were detected through wet chemical extraction (Fig. 2), and no new phases were detected by XRD (Fig. 7). These results suggest that the NO_x binding mechanism might be surface adsorption, which could be detected and measured by the wet chemical extraction used in this study. Since both AFm phases have similar morphologies and surface features [32,33], the results further indicate that the anion exchange process, which was observed in AFm-SO_4 phase, may not occur in the carbonated AFm phase.

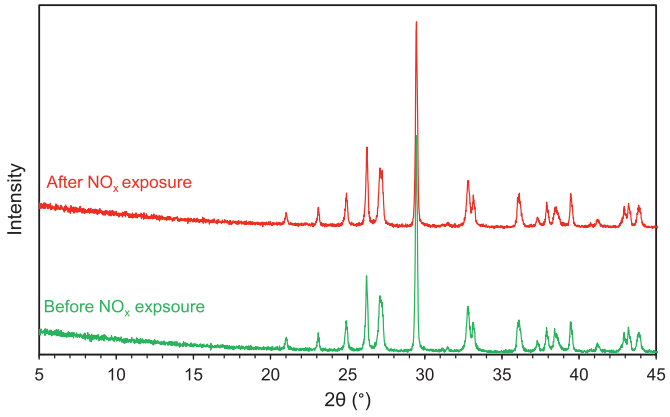

Fig. 6. No new peaks were observed in the XRD patterns of calcite before (control) and after NO_x exposure, suggesting that the formed $Ca(NO_2)_2$ and/or $Ca(NO_3)_2$ could be highly hygroscopic and undetectable by XRD.

4. Discussion

4.1. Transiency and permanency of NO_x binding

Since C-S-H and $Ca(OH)_2$ are the main phases in OPC-based cementitious materials, the transient binding mechanisms of these two phases confirm our previous observation that NO_x binding in OPC-based cementitious materials is largely transient and susceptible to water-based wet chemical extraction [5]. Additionally, the fact that NO_2^- and NO_3^- ions in both C-S-H or calcium nitrite/nitrate are susceptible to water-based chemical extraction suggests high mobility of the produced nitrate/nitrite, which also helps partially explain the previous observations that the NO_x binding capacity could be recovered after the samples were subjected to water, such as during rainfall [4,7]. However, the transient NO_x binding could be problematic as the nitrites and nitrates could be released back to groundwater, aquatic and forest systems, or into agricultural systems [34]. For example, certain amounts of NO_2, which is produced in the photocatalytic process, could be released back to the environment [35,36]. In addition, the transient NO_x binding could potentially be harmful to the photocatalytic TiO_2-modified cementitious materials. For example, the nitrous and nitric acids that are formed through photocatalytic reactions could cause decomposition of the C-S-H and $Ca(OH)_2$ phases and compromise the surface integrity and mechanical properties of the material [37].

Based on Section 3.3, the NO_x binding in aluminate rich phases such as AFm appears to be more permanent, providing a potential pathway to overcome these concerns and enhance the sustainability of NO_x sequestration. Therefore, to improve the potential for permanent NO_x binding, calcium aluminate cement (CAC) with higher aluminate content (compared to OPC) could be advantageous for this application. Our previously study [6] has demonstrated that NO_x uptake through photocatalytic reactions in CAC-based cementitious materials can only be partially recovered by water-based wet chemical extraction. The results further validate the anion exchange process in NO_x binding within AFm-SO_3 phase that is observed in this study.

4.2. Effect of carbonation on NO_x binding

This study has shown that the carbonation of cementitious material

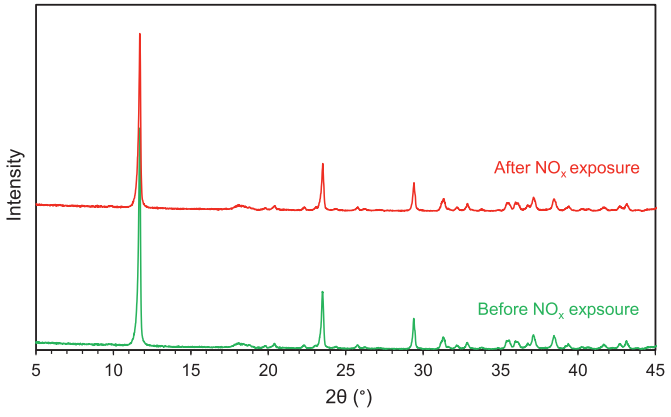

Fig. 7. No new peaks were observed in the XRD patterns of AFm-CO_3 phases before (control) and after NO_x exposure, suggesting that the anion exchange process, which has been observed in AFm-SO_4 phase (Fig. 6), may not occur in AFm-CO_3.

could positively impact NO_x sequestration. According to the Fig. 2, the uptake capacity of $CaCO_3$ phases is three times that of C-S-H, suggesting that carbonation could be a potential pathway to increase NO_x binding capacities in cementitious materials. Kaja et al. [15] have observed a similar enhancement of NO_x degradation in a carbonated portlandite-rich mortar and concluded that the carbonation of calcium-bearing phases increases the formation of capillary pores resulting in enhanced NO_x degradation. Based on the results from Section 3.4, this phenomenon could be further explained by including the additional heterogeneous NO_x binding pathway of $CaCO_3$, which increases the potential chemical sink for NO_x, especially when the reactions are not only on the surface of the $CaCO_3$ particles but also occur in bulk mixtures [9]. Moreover, since carbonation usually initiates from the concrete surfaces, this favors NO_x uptake as the surfaces are also directly exposed to NO_x. The released CO_2 from the reactions (Eqs. (7) and (8)) could carbonate other uncarbonated $Ca(OH)_2$ phases, resulting in further enhanced NO_x binding capacity. Therefore, the carbonation of cement-based materials could potentially increase the material's NO_x sequestration capacity even with low surface area and lack of interlayer water and pore solution-containing pores. However, as the mass of carbonated C-S-H, $Ca(OH)_2$, and $CaCO_3$ are not the same in cementitious materials, more CO_2 uptake is possible by the carbonation of $Ca(OH)_2$ than C-S-H and composition can be adjusted to enhance binding. Further studies are needed to quantify and compare the NO_x uptake potentials between uncarbonated and carbonated phases based on their mass fractions and degree of carbonation. Additionally, the effect of re-released CO_2 on the sustainability concerns should be examined in the future study.

The carbonation of AFm phases, as shown in Section 3.5, could potentially inhibit the anion exchange process and result in a transient NO_x binding. According to Balonis [30,38], NO_2^- and NO_3^- should have a greater thermodynamic occupation preference than CO_3^{2-}. However, this conclusion was based on the interaction of ionic solution and solid phases [30,38]. As demonstrated in this study, without an abundant presence of water, the difference in the thermodynamic occupation preference between NO_2^- and NO_3^- ions and CO_3^{2-} ions may not be significant, thus preventing the anion exchange. Therefore, the water molecules that are associated with carbonated AFm phases are critical for the anion exchange process to occur and thereby maintain the benefits of AFm-SO_4 phases.

5. Conclusion and future perspectives

In this study, five cementitious phases, calcium silicate hydrate, portlandite, mono-sulfoaluminate, calcite, and mono-carboaluminate were tested for their NO_x uptake, toward understanding their binding capacity and mechanisms. A combined method of wet chemical extraction, UV–vis spectrophotometry, and ion chromatography was used to quantify NO_x uptake and to delineate between nitrite and nitrate update. Together with XRD analysis, the NO_x sequestration mechanisms were examined. The effect of carbonation on NO_x binding was examined by comparing uncarbonated phases with carbonated ones. With this information on NO_x capacities and binding mechanisms for each cementitious phase, this study could provide guidelines for engineers and scientists to properly design a cement-based material that has a desired chemical composition and microstructural features for enhanced NO_x sequestration. Some key insights are summarized as follows.

1. Among uncarbonated phases, C-S-H shows the highest NO_x uptake capacity. The NO_2^- and NO_3^- produced as a result of NO_x conversion either adsorb on the surface of the C-S-H phase or dissolve in the pore solution. The NO_x conversion may not occur in $Ca(OH)_2$ phases due to the environmental conditions used in this study (relative low temperature and relative humidity). The NO_2^- and NO_3^- ions interact with the AFm-SO_4 phases by substituting for sulfate ions to form AFm-NO_2/NO_3 phases, which could be detected by XRD.
2. For carbonated phases, $CaCO_3$ exhibits an improved NO_x sequestration capacity compared to uncarbonated phases, with a NO_x uptake capacity *three times* higher than that of C-S-H. This higher capacity could be attributed to the reactions between the produced nitrite and nitrate and the $CaCO_3$ and can occur both on the surface of the $CaCO_3$ particles and in the bulk mixtures. However, the formed $Ca(NO_2)_2$ and $Ca(NO_3)_2$ could not be detected by XRD, possibly due to the poor crystallinity of the formed products. The carbonation of AFm-SO_4 phases could potentially inhibit the anion exchange process that was observed in uncarbonated AFm-SO_4 phases; and NO_x likely absorb on the surface of the solids of AFm-CO_3.

Based on the results and conclusion, the following future studies are recommended. Additional studies need to be performed on the C-S-H with different Ca/Si ratio. This study has revealed that both temperature and water play an important role in NO_x sequestration capacities and pathways in hydrated cementitious phases. In concrete infrastructure, a major source of water is the relative humidity in the environment. Therefore, additional experiments are needed to confirm the impact of temperature and relative humidity on NO_x sequestration by cementitious phases. As aluminate-bearing phases could potentially provide a more permanent NO_x binding, future research could consider including other common aluminate phases in cementitious materials such as C-A-S-H, AH_3, C_3AH_6, and C_2AH_8. As amorphous phases (e.g., amorphous $CaCO_3$ and amorphous silica gel) also exist in concrete, these phases should also be studied in the future to understand their binding mechanisms relative to the crystalline phases examined here. More importantly, it remains unclear how these binding mechanisms occur in hydrated cementitious phases: whether they occur simultaneously or sequentially. In addition, it is also important correlate the NO_x uptake potential with the surface area and pore structure. Since nitrite and nitrate can be used at the steel interface to improve the corrosion resistance of steel-reinforced concrete, a future study could be carried out to understand and quantify the potential resistance against chloride-induced corrosion by tailoring cementitious materials with different C-S-H, $CaCO_3$, and AFm-SO_4 content.

CRediT authorship contribution statement

Qingxu Jin: Conceptualization, Investigation, Methodology, Validation, Formal analysis, Data Curation, Visualization, Project administration, Writing - Original Draft, Writing - Review & Editing.

Samuel N. Lucas: Investigation, Data Curation, Writing - Review & Editing.

Yuanzhi Tang: Methodology, Resources, Writing - Review & Editing.

Kimberly E. Kurtis: Conceptualization, Resources, Project administration, Writing - Review & Editing, Supervision, Funding acquisition.

Declaration of competing interest

None.

Acknowledgements

The authors gratefully acknowledge the financial support from the National Science Foundation (NSF) under Grant No. CMMI-1362843 and EEC-1757579. Any opinions, findings, and conclusions or recommendations expressed in this material are those of the author(s) and do not necessarily reflect the views of the NSF. The authors would like to thank Monday Okoronkwo from Chemical and Biochemical Engineering Department at Missouri University of Science and Technology and the Laboratory for the Chemistry and Construction Materials at University of California, Los Angeles for the preparation of AFm-SO_4 and AFm-CO_3 phases.

References

[1] NO_x: How Nitrogen Oxides Affect the Way We Live And Breathe, Office of Air Quality Planning and Standards, Research Triangle Park, NC 27711, 1998.

[2] H.J.H. Brouwers, M.M. Ballari, M. Hunger, G. Hu, NO_x photocatalytic degradation employing concrete pavement containing titanium dioxide, Appl. Catal. B Environ. 95 (2010), https://doi.org/10.1016/j.apcatb.2010.01.002.

[3] M.M. Ballari, M. Hunger, G. Hüsken, H.J.H. Brouwers, Modelling and experimental study of the NO x photocatalytic degradation employing concrete pavement with titanium dioxide 151, 2010, https://doi.org/10.1016/j.cattod.2010.03.042.

[4] J. Chen, C.S. Poon, Photocatalytic cementitious materials: influence of the microstructure of cement paste on photocatalytic pollution degradation, Environ. Sci. Technol. 43 (2009), https://doi.org/10.1021/es902359s.

[5] Q. Jin, E.M. Saad, W. Zhang, Y. Tang, K.E. Kurtis, Quantification of NO_x uptake in plain and TiO_2-doped cementitious materials, Cem. Concr. Res. 122 (2019) 251–256, https://doi.org/10.1016/J.CEMCONRES.2019.05.010.

[6] Q. Jin, S.L. Hordern, Y. Tang, K.E. Kurtis, NO_x sequestration by calcium aluminate cementitious materials, Cem. Concr. Res. 142 (2021), 106381.

[7] J. Chen, C.S. Poon, Photocatalytic construction and building materials: from fundamentals to applications, Build. Environ. 44 (2009), https://doi.org/10.1016/j.buildenv.2009.01.002.

[8] Y. Hendrix, A. Lazaro, Q. Yu, J. Brouwers, Titania-silica composites: a review on the photocatalytic activity and synthesis methods, World J. Nano Sci. Eng. 05 (2015) 161–177, https://doi.org/10.4236/wjnse.2015.54018.

[9] V.H. Grassian, Chemical reactions of nitrogen oxides on the surface of oxide, carbonate, soot, and mineral dust particles: implications for the chemical balance of the troposphere, 2002, https://doi.org/10.1021/JP012139H.

[10] B.Y. Lee, A.R. Jayapalan, M.H. Bergin, K.E. Kurtis, Photocatalytic cement exposed to nitrogen oxides: effect of oxidation and binding, Cem. Concr. Res. 60 (2014), https://doi.org/10.1016/j.cemconres.2014.03.003.

[11] M. Horgnies, I. Dubois-Brugger, E.M. Gartner, NO_x de-pollution by hardened concrete and the influence of activated charcoal additions, Cem. Concr. Res. 42 (2012) 1348–1355, https://doi.org/10.1016/J.CEMCONRES.2012.06.007.

[12] C.H. Nelli, G.T. Rochelle, Nitrogen dioxide reaction with alkaline solids, Ind. Eng. Chem. Res. 35 (1996) 999–1005, https://doi.org/10.1021/ie950117+.

[13] Q. Jin, Fundamental Understanding of NO_x Sequestration Capacity And Pathways in Nano-TiO_2 Engineered Cementitious Materials, Georgia Institute of Technology (2019).

[14] L. Yang, A. Hakki, F. Wang, D.E. Macphee, Photocatalyst efficiencies in concrete technology: the effect of photocatalyst placement, Appl. Catal. B Environ. 222 (2018) 200–208, https://doi.org/10.1016/j.apcatb.2017.10.013.

[15] A.M. Kaja, H.J.H. Brouwers, Q.L. Yu, NO_x degradation by photocatalytic mortars: the underlying role of the CH and C-S-H carbonation, Cem. Concr. Res. 125 (2019), https://doi.org/10.1016/j.cemconres.2019.105805.

[16] P. Hewlett, Lea's Chemistry of Cement And Concrete, 2004, https://doi.org/10.1016/B978-0-7506-6256-7.50031-X.

[17] A.J. Allen, J.J. Thomas, H.M. Jennings, Composition and density of nanoscale calcium – silicate – hydrate in cement, 2007, https://doi.org/10.1038/nmat1871.

[18] E. L'Hôpital, B. Lothenbach, G. Le Saout, D. Kulik, K. Scrivener, Incorporation of aluminium in calcium-silicate-hydrates, Cem. Concr. Res. 75 (2015), https://doi.org/10.1016/j.cemconres.2015.04.007.

[19] T. Matschei, B. Lothenbach, F.P. Glasser, The AFm phase in Portland cement, Cem. Concr. Res. 37 (2007), https://doi.org/10.1016/j.cemconres.2006.10.010.

[20] ISO 22197-1:2007, Fine ceramics (advanced ceramics, advanced technical ceramics) – test method for air-purification performance of semiconducting photocatalytic materials – part 1: removal of nitric oxide (n.d.), https://www.iso.org/standard/40761.html. (Accessed 22 September 2018).

[21] JIS R 1701-1, Fine Ceramics (Advanced Ceramics, Advanced Technical Ceramics)—Test Method for Air Purification Performance of Photocatalytic Materials—Part 1: Removal of Nitric Oxide, Japanese Standards Association, Tokyo, Japan, 2004, 24 pp., (n.d.).

[22] P. Hewlett, Lea's Chemistry of Cement And Concrete, Elsevier, 2004.

[23] Q. Jin, M. Faraldos, A. Bahamonde, B.H. Zaribaf, K.E. Kurtis, Titania and Silica Nanoparticle-Modified Coatings for Cementitious Materials, ACI Symp. Publ (2019) 97–111, https://doi.org/10.1016/j.cemconcomp.2018.11.016.

[24] J. Li, G. Geng, R. Myers, Y.S. Yu, D. Shapiro, C. Carraro, R. Maboudian, P.J. M. Monteiro, The chemistry and structure of calcium (alumino) silicate hydrate: a study by XANES, ptychographic imaging, and wide- and small-angle scattering, Cem. Concr. Res. 115 (2019) 367–378, https://doi.org/10.1016/J.CEMCONRES.2018.09.008.

[25] J. Li, W. Zhang, K. Xu, P.J.M. Monteiro, Fibrillar calcium silicate hydrate seeds from hydrated tricalcium silicate lower cement demand, Cem. Concr. Res. 137 (2020), 106195, https://doi.org/10.1016/J.CEMCONRES.2020.106195.

[26] X. Zhang, H. Tong, H. Zhang, C. Chen, Nitrogen oxides absorption on calcium hydroxide at low temperature, Ind. Eng. Chem. Res. 47 (2008) 3827–3833, https://doi.org/10.1021/ie070660d.

[27] G. Chen, J. Gao, J. Gao, Q. Du, X. Fu, Y. Yin, Y. Qin, Simultaneous removal of SO_2 and NO_x by calcium hydroxide at low temperature: effect of SO_2 absorption on NO_2 removal, Ind. Eng. Chem. Res. 49 (2010) 12140–12147, https://doi.org/10.1021/ie101594x.

[29] F.P. Glasser, M. Mędala, M. Balonis, Influence of calcium nitrate and nitrite on the constitution of AFm and AFt cement hydrates, Adv. Cem. Res. 23 (2011), https://doi.org/10.1680/adcr.10.00002.

[30] G. Puerta-Falla, M. Balonis, G. Falzone, M. Bauchy, N. Neithalath, G. Sant, Monovalent ion exchange kinetics of hydrated calcium-alumino layered double hydroxides, Ind. Eng. Chem. Res. 56 (2017), https://doi.org/10.1021/acs.iecr.6b03474.

[31] A. Morandeau, M. Thiéry, P. Dangla, Investigation of the carbonation mechanism of CH and C-S-H in terms of kinetics, microstructure changes and moisture properties, Cem. Concr. Res. 56 (2014) 153–170, https://doi.org/10.1016/j.cemconres.2013.11.015.

[32] T. Matschei, B. Lothenbach, F.P. Glasser, in: The AFm phase in Portland cement 37, 2007, pp. 118–130, https://doi.org/10.1016/j.cemconres.2006.10.010.

[33] M.U. Okoronkwo, F.P. Glasser, Compatibility of hydrogarnet, $Ca_3Al_2(SiO_4)_x(OH)_4(3-X)$, with sulfate and carbonate-bearing cement phases: 5–85 °c, Cem. Concr. Res. 83 (2016) 86–96, https://doi.org/10.1016/j.cemconres.2016.01.013.

[34] P. Gundersen, I.K. Schmidt, K. Raulund-Rasmussen, Leaching of nitrate from temperate forests - effects of air pollution and forest management, Environ. Rev. 14 (2006) 1–57, https://doi.org/10.1139/a05-015.

[35] R. Sugrañez, J.I. Álvarez, M. Cruz-Yusta, I. Mármol, J. Morales, J. Vila, L. Sánchez, Enhanced photocatalytic degradation of NO_x gases by regulating the microstructure of mortar cement modified with titanium dioxide, Build. Environ. 69 (2013) 55–63, https://doi.org/10.1016/j.buildenv.2013.07.014.

[36] C. Cárdenas, J.I. Tobón, C. García, J. Vila, Functionalized building materials: photocatalytic abatement of NO x by cement pastes blended with TiO 2 nanoparticles 36, 2012, https://doi.org/10.1016/j.conbuildmat.2012.06.017.

[37] T. Ibusuki, Cleaning atmospheric environment (photocatalytic activities of TiO_2), in: M. Kaneko, I. Okura (Eds.), Photocatal. Sci. Technol, Springer, Berlin Heidelberg, 2010, p. 143.

[38] G. Falzone, M. Balonis, G. Sant, X-AFm stabilization as a mechanism of bypassing conversion phenomena in calcium aluminate cements, Cem. Concr. Res. 72 (2015), https://doi.org/10.1016/j.cemconres.2015.02.022.